Venusian Applications of 3D Convection Modeling

Timary “Annie” Bonaccorso

Jet Propulsion Laboratory, California Institute of Technology

Major: Chemistry

USRP Summer Session

15 August 2011

Venusian Applications of 3D Convection Modeling

Timary "Annie" Bonaccorso[1]
Brown University, Providence, RI, 02912

This study models mantle convection on Venus using the 'cubed sphere' code OEDIPUS, which models one-sixth of the planet in spherical geometry. We are attempting to balance internal heating, bottom mantle viscosity, and temperature difference across Venus' mantle, in order to create a realistic model that matches with current planetary observations. We also have begun to run both lower and upper mantle simulations to determine whether layered (as opposed to whole-mantle) convection might produce more efficient heat transfer, as well as to model coronae formation in the upper mantle. Upper mantle simulations are completed using OEDIPUS' Cartesian counterpart, JOCASTA. This summer's central question has been how to define a mantle plume. Traditionally, we have defined a hot plume the region with temperature at or above 40% of the difference between the maximum and horizontally averaged temperature, and a cold plume as the region with 40% of the difference between the minimum and average temperature. For less viscous cases (10^{20} Pa·s), the plumes generated by that definition lacked vigor, displaying buoyancies 1/100th of those found in previous, higher viscosity simulations (10^{21} Pa·s). As the mantle plumes with large buoyancy flux are most likely to produce topographic uplift and volcanism, the low viscosity cases' plumes may not produce observable deformation. In an effort to eliminate the smallest plumes, we experimented with different lower bound parameters and temperature percentages.

Nomenclature

α	=	Coefficient of Thermal Expansion	$3 \cdot 10^{-5}$	K^{-1}
η_0	=	Bottom Viscosity	--	Pa·s
η_{surf}	=	Surface Viscosity	--	Pa·s
κ	=	Coefficient of Thermal Diffusivity	10^{-6}	m^2/s
ρ	=	Mantle Density	3500	kg/m^3
d	=	Thickness of the Layer	--	m
$avis$	=	Nondimensional (ND) Temperature-Dependence of Viscosity	--	--
H	=	Volumetric Heating Rate	--	W/m^3
H_s	=	ND Internal Heating Rate	--	--
P_f	=	Heat Flux Lower Bound	--	W/m^2
q	=	Heat Flux	--	W/m^2
R	=	Ideal Gas Constant	8.314	J/mol-K
Ra	=	Surface Rayleigh Number	--	--
ΔT	=	Temperature Difference Across Layer	--	K
T	=	Temperature	--	K
T_{avg}	=	Average Temperature	--	K
T_m	=	Convective Mantle Temperature	--	K
u_z	=	Vertical Velocity	--	m/s

I. Introduction

Venus, Earth's closest planetary neighbor, is also the most "Earth-like" planet, particularly in terms of size, composition, and acceleration due to gravity. However, there is one striking geological difference between the two planets: unlike Earth, Venus shows no evidence of plate tectonics; instead, Venus' lithosphere forms a slow-moving, highly viscous lid, or a stagnant lid regime.[1]

[1] USRP Research Intern, Geophysics and Planetary Geosciences, Jet Propulsion Laboratory, National Aeronautics and Space Administration and California Institute of Technology.

Two different types of mantle upwellings have been observed on Venus: large scale "hotspots," which display volcanoes and topographic rises similar to those observable in Hawaii, and smaller coronae, features unique to Venus.[1] Large Venusian upwellings, similar to the terrestrial hotspots that form the Hawaiian islands, tend to have a diameter around 1000 to 2000 km, while coronae tend to be around 250-500 km in diameter.[2] Convection in the mantle creates these two types of upwellings, though how the two different types are formed is not well understood. Large hotspots appear to begin deep in the mantle at the core-mantle boundary, while coronae are thought to form only in the upper mantle.

Whole mantle plumes refer to the mantle upwellings that result in large-scale hotspots.[3,4] Hot whole mantle plumes are generated at the hot thermal boundary layer (TBL), also referred to as the 'bottom thermal boundary layer,' and rise through the convective part of the mantle toward the lithosphere and, eventually deform the surface. Internal heating due to the decay of long-lived radiogenic elements is transferred to the surface by advection of heat in the convective domain and conduction in the highly viscous lid (Fig. 1). Above the hot thermal boundary layer lies the convective layer of the mantle, where horizontally averaged temperature is adiabatic and vertical temperature gradients are small. The intersection of the mantle's advection and diffusion curves marks where the convective part of the mantle ends and the conductive lid begins. The cold thermal boundary layer, or top thermal boundary layer, is where the downwelling cold plumes form. Between the top thermal boundary layer and the surface of the planet is the conductive lid, where heat transfer is dominated by conduction rather than convection. The lithosphere of a planet indicates whether plate tectonics exist. Evidence suggests that Venus has no plate tectonics, but rather alternates through periods of resurfacing and stagnant lid regimes.

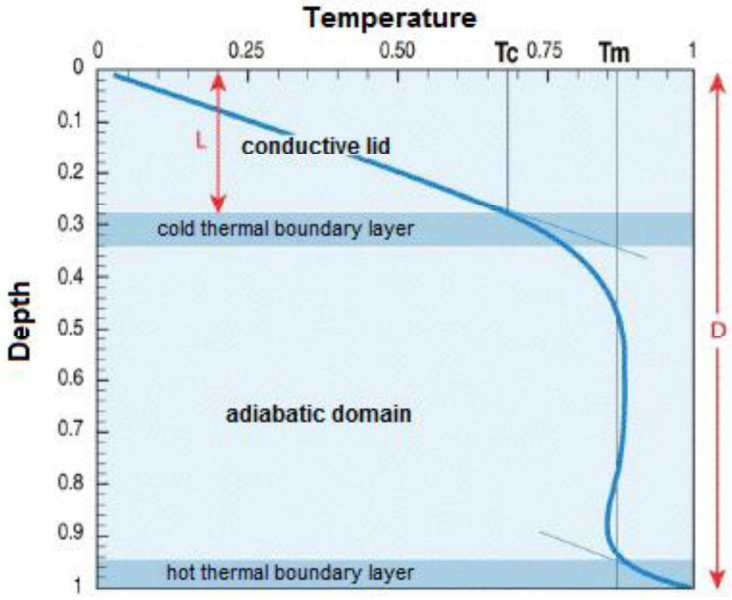

Figure 1. Layers of the convective domain.

Venus' lack of plate tectonics and high surface temperature means that we cannot simply rely on convection models designed for Earth to explain the mantle upwellings that create volcanoes and coronae. A different model must be used to simulate mantle convection on Venus.

The 3D spherical code OEDIPUS, developed by Gael Choblet and his colleagues at the Université de Nantes, France, was used to model whole mantle and lower mantle convection on Venus.[5] Previous studies have modeled heat flux and convection in planetary mantles, but these were either in Cartesian coordinates or were better suited to isoviscous fluids than Venus' mantle, which has temperature-dependent viscosity.[6,7] Spherical geometry, as opposed to Cartesian, is particularly important for modeling plumes that stem from the core-mantle boundary, due to the shape of the planet. OEDIPUS, also referred to as the "cubed sphere" model, is a finite-volume formulation Fortran code which models one sixth of the planet at a time.[5] As only one sixth of the planet is modeled at a time, our results must be multiplied by six to achieve values relevant to the whole of Venus. We used this code in an effort to generate ~1.5 hot plumes per sixth of the sphere, so as to produce the estimated nine volcanic areas observed on Venus.[2]

To model upper mantle convection, a related code is employed. As the upper mantle is only around 740 km thick (742 for ease of calculation), whereas the radius of the entire mantle is 2932 km, the upper mantle can be approximated as a box, as opposed to one-sixth of the sphere. The x- and y-dimensions do not change greatly with increasing depth over a small distance, so it is possible to use OEDIPUS' Cartesian counterpart, JOCASTA, to model upper mantle convection and coronae formation. One area of Venus that JOCASTA is being used to model is Themis Regio, a corona-dominated area in the planet's southern hemisphere. It appears to have thirteen coronae directly on the topographic rise, and twelve in the immediately surrounding area. Upper mantle simulations are useful both to model the formation of coronae and, when used in conjunction with lower mantle models, to examine the feasibility of layered, as opposed to whole-mantle, convection.

Both OEDIPUS and JOCASTA are run on the supercomputer Pleiades, which is located at NASA AMES in Moffett Field, California. Output from both 3D convection codes is analyzed in MATLAB using programs produced by my intern predecessors and myself. These codes allow us to visualize plume formation in both 2D and 3D. MATLAB scripts are invaluable for interpreting the strings of data output by each Fortran code into meaningful results.

II. Background

This is my second summer working with Drs. Christophe Sotin and Sue Smrekar to model mantle convection on Venus. Last summer, I mainly focused on whole mantle convection, though I also completed two lower mantle simulations. For my whole mantle runs, I attempted to balance internal heating and temperature difference between the core-mantle boundary and the surface in order to create a realistic computer model of Venus' mantle that matched with current observations of the planet. I also had hoped to begin upper mantle simulations in Cartesian coordinates. Unfortunately, we did not switch over to the AMES supercomputer until late in the summer and by time we were set up to use the supercomputer at AMES (which, unlike the JPL supercomputer I had used earlier in the summer, has the processing power necessary for the Cartesian code to converge) the supercomputer at the Université de Nantes in France, from which we needed to retrieve certain files in order to run JOCASTA, was undergoing serious maintenance and would not be available until after the completion of my internship. This summer, I focused on upper and lower mantle simulations, while my partner intern completed the whole mantle runs.

III. Objectives

I had three main objectives this summer – not all of them anticipated at the beginning of the summer. I expected to spend the bulk of my time this summer on upper and lower mantle modeling. With regards to upper mantle modeling, my goals were to get JOCASTA set up to run on the AMES supercomputer and to compare plume formation over several JOCASTA runs to the coronae formations observed on Venus' surface – particularly at Themis Regio. We hoped to pair upper mantle modeling, my first objective, with lower mantle modeling, my second, to examine the possibility of layered convection on Venus. My third and most unexpected goal this summer was to redefine how plumes are counted in the MATLAB output for whole mantle OEDIPUS runs. In the cases completed by previous interns with large values of nondimensional internal heating (H_s=2.5-10) and low bottom viscosities (10^{20} as opposed to 10^{21} Pa·s), the plumes generated by our traditional methods lacked realistic buoyancies. Our goal was to find a new definition that decreased the number of plumes (and thus increased the buoyancy of each plume) for the problem cases without eliminating all plumes for the cases with higher bottom viscosity.

IV. Method

A. 3D Convection Codes

Though output from OEDIPUS and JOCASTA are in different 3D coordinate systems, the input to each code is very similar. The most important input parameter in the theory of convection is the Rayleigh number. A lower Rayleigh number indicates less strong convection. The input used for both lower and upper mantle modeling is the surface Rayleigh number:

$$Ra = \frac{\alpha \rho g (\Delta T)(d)^3}{\kappa \eta_{surf}} \tag{1}$$

which incorporates several key features of each run: the surface viscosity, thickness of the layer, and temperature difference across the layer. Surface viscosity depends on the bottom viscosity (found at the core-mantle boundary for whole or lower mantle runs, and found at the base of the upper mantle for upper mantle runs) and the *avis*, or temperature dependence of the viscosity:

$$\eta_{surf} = \frac{\eta_0}{e^{-avis}} \tag{2}$$

Therefore, the surface Rayleigh number is also dependent on bottom viscosity and *avis*. The three parameters that we regularly change in the Rayleigh number equation are ΔT, *avis*, and η_0. The layer thickness is always 2932000 m for whole, 2190000 m for lower, and 742000 m for upper mantle modeling, and α, κ, ρ, and g are constants.

The other key inputs to both OEDIPUS and JOCASTA are the boundary conditions and nondimensional internal heating value. For OEDIPUS, boundary conditions can be either free slip or no slip at the base of the layer (they are always no slip at the top); JOCASTA offers slightly different options: no slip at top and bottom, free slip at the top and bottom, and no slip at the top with a free slip base. No slip indicates that the velocity becomes zero at the boundary; free slip allows the velocity to be any value at the boundary. So far, all JOCASTA runs have been run with the no slip boundary condition at both the top and bottom of the layer.

Nondimensional internal heating due to radioactive decay of materials in the planet's core is another possible input for both OEDIPUS and JOCASTA, though the MATLAB codes used to analyze JOCASTA output would have to be modified to account for internal heating. Internal heating is currently implemented only for whole and lower mantle simulations run on OEDIPUS. Internal heating is calculated as follows:

$$H_s = \frac{\rho H d}{k(\Delta T)} \tag{3}$$

Internal heating indicates the amount of heat released per kilogram of mantle material, and greatly influences the thicknesses of the thermal boundary layers, as well as the number of plumes.

B. MATLAB

OEDIPUS and JOCASTA output 3D arrays of nondimensional temperature, flux and velocity, as well as indicate the nondimensional time the run has completed. It is difficult to meaningfully analyze long strings of data; visualization of the data is paramount to understanding our results. MATLAB both enables the dimensionalization of the output and models plume formation in 2D and 3D. MATLAB is adequate for 3D visualization of Cartesian plume formation, but has difficulty fully realizing the 'cubed sphere' output from OEDIPUS. The core-mantle boundary is not wide enough in the x and y directions. To model plume formation in 3D, we turn to visualization software developed at Ames (Fig. 2).

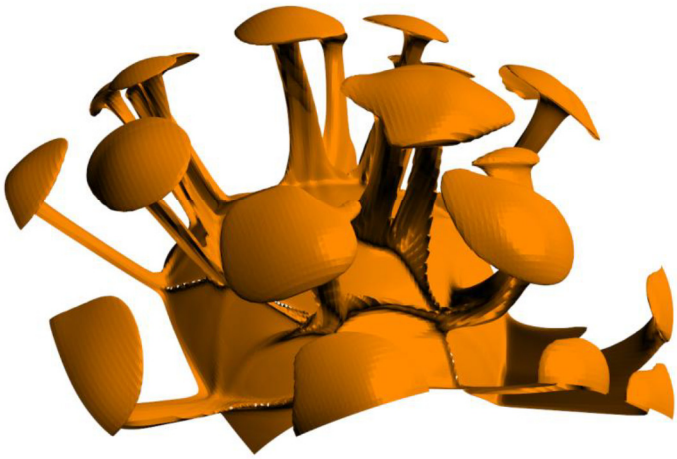

Figure 2. 3D visualization of hot plumes in 1/6th of the sphere.

In our attempts to redefine plumes this summer, we experimented with various heat flux criteria. Heat flux was calculated in the manner of Zhong's 2005 paper: [8]

$$q = u_z(T - T_{avg}) \tag{4}$$

To achieve units of W/m^2, the density of the material and its specific heat are multiplied by the above result. In various forms, heat flux was used as a lower bound for plume formation when analyzing the size of the anomalies formed at mid-mantle.

V. Results

A. Upper Mantle Modeling

During my internship last summer, I had hoped to begin Cartesian runs on JOCASTA, only to be stymied by the extensive maintenance being performed on the Nantes supercomputer. This summer, thankfully, I was able to obtain the restart files and makefiles I needed to begin upper mantle runs.

The restart files I received were nearly at steady state for a*vis* 15, a surface Rayleigh number of 2.8089, no internal heating, and no slip boundary conditions. The model was being run with these parameters to simulate a depth of 50 km into the ice on Europa, but when I solved the surface Rayleigh number for Venusian parameters and a temperature difference of 915 K (found by subtracting 225 K, an imagined lower mantle temperature change, from

1140 K, our go-to temperature difference for whole mantle simulations), I generate a bottom viscosity of $3.8 \cdot 10^{19}$ Pa•s. This bottom viscosity is certainly on the lower end of the range of possible viscosities, but still reasonable.

One of the major goals of upper mantle modeling, beyond using both lower and upper mantle simulations to determine the feasibility of layered convection, is to model the formation of coronae. After plotting the number of plumes using 40% of the maximum and minimum temperature difference at mid-depth, I was able to calculate the distance between the coronae formed using this JOCASTA simulation. As the grid is 256 by 256 and the aspect ratio (horizontal to vertical distance) is 2, 256 grid points is equal to 1484 km (twice the radial distance from surface to upper-lower mantle boundary). I was able to use this conversion find the distance from the center of one corona to another. Plume 1 is 95 grid points, or 549 km away from Plume 6, and the other plumes are similarly spaced from their nearest plumes. Figure 3 illustrates the spacing between the nearest coronae and labels each hot plume with a number, and Table 1 in the Appendix lists the distance from each corona to the other five.

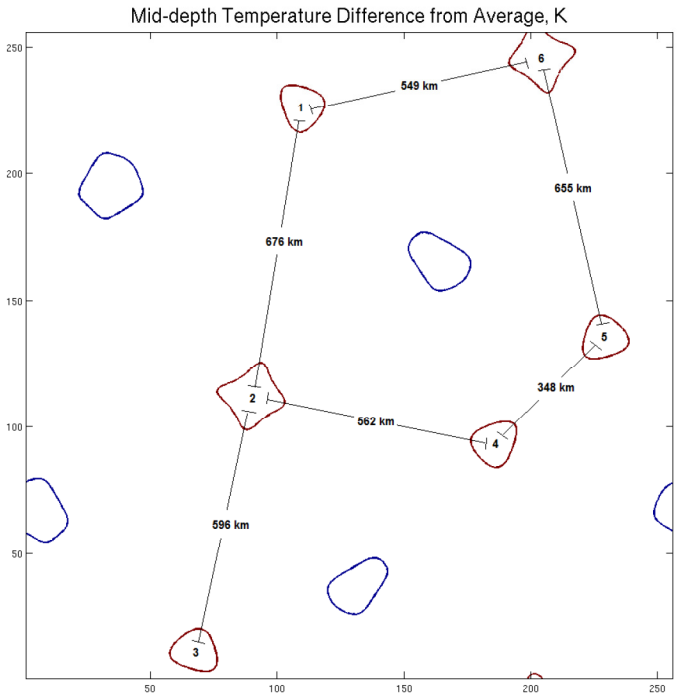

Figure 3. Coronae distances.

I have since increased the *avis* from 15 to 17, keeping all other input values the same. This gives a surface Rayleigh number of 0.3801. That run has not yet reached steady state. The goal is to reach *avis* 20, the *avis* at which most whole mantle runs are performed, before changing other input parameters. The code does not converge properly if too many variables are changed at once, so it is best to increase *avis* to the desired value before changing the bottom viscosity or any other parameters.

B. Lower Mantle Modeling

I have begun three runs for lower mantle modeling. The first run I began had an *avis* of 20, a free slip boundary condition, a bottom viscosity of 10^{20} Pa·s, a nondimensional internal heating value of 10 and a temperature difference of 500 K (see Table 2 for full input). I chose restart files that had a bottom viscosity of 10^{20} Pa·s, temperature difference of 1140 K, free slip condition, and an internal heating value of 10, thinking that if I only changed the temperature difference, the code would reach steady state faster. Unfortunately, these restart files are run on a grid that is 256x128x128, as opposed to the 128^3 grid that I had used for whole mantle runs in the past, and this greater grid resolution has taken an incredibly long time to reach steady state (more than 20 days of runtime on the AMES supercomputer and counting). The is equivalent to Venus' lower mantle taking more than $1.3 \text{x} 10^{10}$ years to run, which is more than three times the age of the solar system! This run is now a low priority, both due to its incredible runtime and the fact that 500 K now seems to be too large a temperature difference. For our next run, we chose a temperature difference of less than half of the temperature difference of this run.

Choosing the input parameters for the next lower mantle run was surprisingly difficult. We wanted to be able to compare upper and lower mantle runs to whole mantle simulations, and for this, we needed to reconsider both our *avis* and our internal heating inputs. *Avis* is calculated as such:

$$avis = \frac{Q(\Delta T)}{RT_m^2} \tag{5}$$

To compare my new lower mantle runs to the whole mantle runs at *avis* values of 20, I used this formula to equate one *avis* with another. As Q and R are constant, the formula approximates the following:

$$avis_{new} = \frac{avis_{old}(\Delta T_{\text{new}})}{\Delta T_{\text{old}}} \tag{6}$$

If avis_{old} = 20, ΔT_{new} = 225 K, and ΔT_{old} = 1140 K, we find that $avis_{new}$ = 4. Lower mantle runs at avis 4 are directly comparable to whole mantle runs at avis 20.

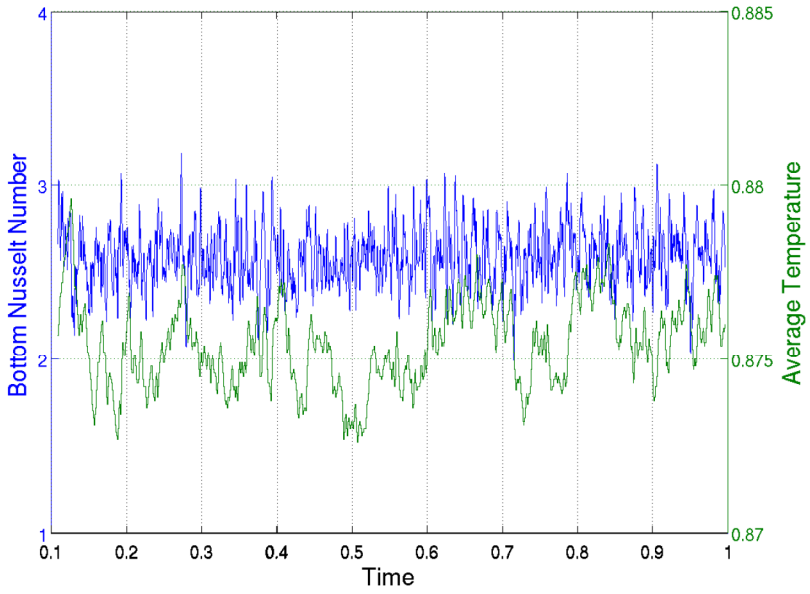

Figure 4. *Avis* = 4, H_s = 18. If the run were converging to steady state, both average nondimensional temperature and bottom Nusselt number would be nearly constant over time.

We chose to compare internal heating to our previous lower mantle case with a temperature difference of 500 K and an internal heating value of 10. I solved Eq. 3 for H for that lower mantle case, and then used that value of H to determine that our H_s value for this lower mantle simulation should be 18.

Unfortunately, this run does not seem to have converged, as I used *avis* = 20 restart files. As evidenced in Fig. 4, neither the nondimensional temperature nor the Nusselt number has become constant over a period of nondimensional time, indicating that the run is not achieving steady state. I have begun a third run with a temperature difference of 225 K and no internal heating, using *avis* = 5 restart files in the hopes that this will converge more easily. The next intern to work on this project will slowly increase internal heating to the desired H_s = 18 result.

C. Plume Definitions

Since last summer, much progress has been made regarding whole-mantle convection modeling. When I left last summer, I had been steadily decreasing nondimensional internal heating from Hs=10 down to Hs=1.25. The intern who worked on this project last fall and who has also returned to work this summer completed runs from Hs=1.25 to 10 using a free slip boundary as opposed to the no slip boundary I had used. He also completed runs with a bottom viscosity of 10^{20} Pa·s, as opposed to the 10^{21} Pa·s that my intern predecessors and I had used (see Table 3 for the input parameters for Runs A-D). Though the intern's runs generated many more plumes than desired, the plumes also lacked vigor. The buoyancy of hot plumes in the low viscosity cases were less than 1/100th of those found in previous simulations with greater bottom viscosity. This inspired me to begin the difficult task of redefining how plumes should be counted. I wrote almost ten different MATLAB codes in an effort to find the plume definition that best fit all of our results.

The traditional method with which I had been measuring plumes was to find the maximum and minimum temperatures at mid-depth, and to use these to determine the most vigorous and least vigorous plume ('Method 1' in Table 4). Hot plumes were any temperature anomaly with a temperature difference greater than 40% of the maximum temperature minus the average temperature across the layer, and cold plumes were any anomaly with a temperature difference greater than 40% of the minimum temperature minus the average. For full details of the number of plumes generated for several cases over different plume criteria, see Table 4.

My second plume definition mirrored the traditional method, except that plumes were identified by having 40% of the maximum or minimum velocity difference across the layer ('Method 2'). This method did not significantly change plume numbers or areas and was quickly discarded.

My next goal was to add a lower bound to the 40% temperature contours and 40% velocity contours. As in Ref. 8, I added a heat flux minimum parameter (P_f) in which only plumes which both fit the temperature or velocity

profile, and which had at least 5 or 10% of the heat flux of the strongest hot plume, were counted (temperature – 'Method 3'; velocity – 'Method 4'). Heat flux is calculated using Eq. 4. I also experimented with using 10 or 20% of the maximum and minimum temperatures to define plumes. All of the methods described above still generated lots of weak, small plumes for the low-viscosity cases and eliminated cold plumes for the more "normal" cases with less internal heating and greater viscosity. With my mentors' and fellow intern's help, we decided that 20% was the best percent to use for defining maximum and minimum temperature contours. This percentage created the largest number of plumes with large radii. 10% created more plumes but many were smaller, as small temperature anomalies that previously would have been ignored were counted. 40% allowed fewer plumes to be counted as anomalies required a higher temperature to qualify as a plume. 20% provided a solid upper bound for plume areas and radii.

After ruling out a constraint in which only plumes which both fit the temperature profile and had at least 5-10% of the heat flux of the strongest plume were counted, I turned to a new heat flux lower bound. I next took 5-10% of the total heat flux across the mid-depth layer. When I tried that constraint, it ruled out all plumes – none of the low viscosity plumes had a great enough heat flux to qualify. I eventually lowered it to 0.1% of the total heat flux, and that did give some plumes, but was deemed unrealistic ('Method 5'). Plumes with only 0.1% of a layer's total heat flux are not vigorous enough.

I turned to a new heat flux criterion – only plumes with heat flux several times greater than the average heat flux across the layer, and which also had at least 20% of the minimum or maximum temperature, would qualify ('Method 6'). To determine what value the constant (referred to as P_f in the style of Ref. 8) required, I plotted the number of hot and cold plumes generated for Run C, the least buoyant case, at P_f =1-14, which is the P_f at which all hot plumes disappeared, and used the scaling from the graph to determine an ideal P_f value (Fig. 5). From this graph, it was decided that we would use P_f =10 as our current definition. P_f =10 gave 3 hot plumes and 28.5 cold plumes for Run C, giving an average plume buoyancy of 8.44 kg/s for hot plumes and -54.1 kg/s for cold plumes. While we originally accepted 8.44 kg/s, it is still much less than the average terrestrial plume buoyancy and in reality was still too small. I then tried P_f =15 and P_f =20 for the three low viscosity cases that were at steady state, and they were even more promising. Unfortunately, anything greater than P_f = 5 eliminated all cold plumes (and sometimes all hot plumes, too) from the other cases, so this method was abandoned.

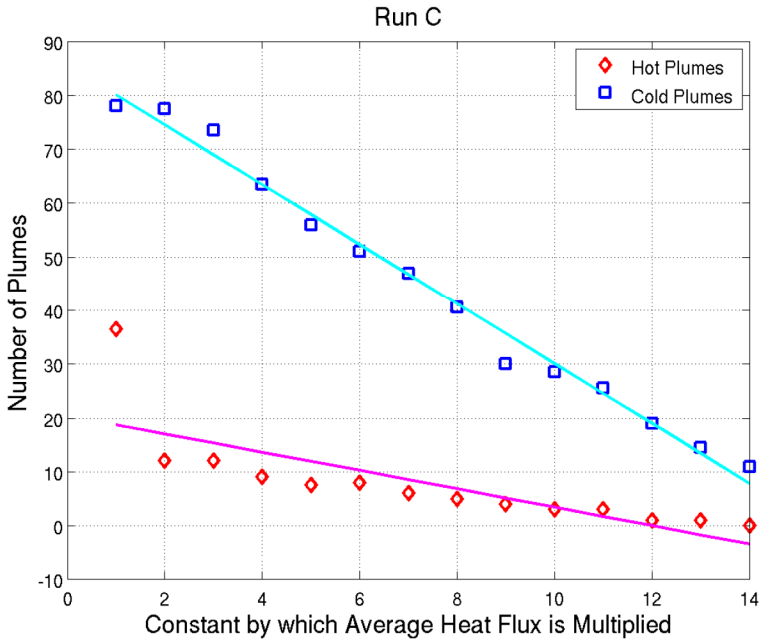

Figure 5. Number of plumes versus P_f.

I next tried a new kind of lower bound – an absolute temperature difference of 50 K ('Method 7'). The hot plumes exhibited excellent results for all seventeen comparison cases, and we almost thought we had found our perfect plume counting method. Unfortunately, the cold plume definition only worked well for the high internal heating, low viscosity cases. In the other cases, it significantly decreased cold plume buoyancies and often eliminated all cold plumes altogether.

I returned to our very first heat flux parameter – five percent of the heat flux of the strongest plume. This time, instead of comparing both hot and cold plume heat fluxes to the strongest hot plume, we required hot plumes to have 5% of the heat flux of the strongest hot plume, and cold plumes to have 5% of the heat flux of the strongest cold plume ('Method 8'). This worked quite well for all of the hot plumes and nearly all of the cold plumes;

however, in a few cases it joined four distinct plumes by a small thread of cold mantle material so that the plume had to be counted as one large plume with a radius of 1500 km, which seems excessively large.

Finally, we returned to our definition of a constant times the average heat flux of the layer. This time, instead of taking the average of the whole layer, I took the average of the hot material to define hot plumes (making every point where there was not a positive temperature difference zero and adding that zero into my average so as to make the lower bound smaller), and an average of the cold material's heat flux to define cold plumes ('Method 9'). The average of the whole layer is larger than the average of either type of plume on its own, because both upwellings and downwellings have positive heat flux. By separating hot and cold plumes, we allowed a few more plumes to qualify that otherwise might have. Thankfully, this definition seems to work when the constant is equal to five. It eliminates some of the many small plumes in the low bottom viscosity cases without removing all the plumes in the higher viscosity cases. When P_f is greater than five, it again eliminates too many plumes for the higher viscosity and lower internal heating cases.

VI. Conclusion

I was pleasantly surprised by the results of this summer's upper mantle research. After our first trial, which wasn't even designed for Venus but rather for Europa, we've already found reasonable coronae distances. The radii are smaller than hoped (~100 km or less), so in the future we will try to generate larger coronae without greatly changing the spacing between hot plumes. We will also work toward increasing *avis* to 20, the value at which we have completed most whole-mantle runs, and then change input parameters to better reflect Venus' bottom viscosity.

Unfortunately, the lower mantle runs that I began this summer are not yet ready for full analysis. My successor will be the one to finish and analyze those runs. After examining the results at *avis* 4 with an H_s of 18, that intern will evaluate whether taking that direction makes sense. We have never completed a run with such a large internal heating and it is very possible that the mantle will be too hot for any plumes to form, so it is quite likely that the next intern will decrease the internal heating present in the lower mantle cases.

Now that an appropriate definition for plumes has been found, it will be interesting to examine how plume formation appears at different depths. All of our old plume definitions took place at mid-depth, but it will be interesting to see how plumes look at the hot thermal boundary layer, cold thermal boundary layer, and the base of the conductive lid. The next intern will analyze the number of plumes, their areas, and their buoyancies to further understand the evolution of Venus' mantle.

Appendix

Table 1. Coronae Spacing for Avis 15 JOCASTA Run.

Plume Number 1	Plume Number 2	Distance (grid points)	Distance (km)
1	2	117	676
	3	219	1,271
	4	154	893
	5	150	872
	6	95	549
2	1	117	676
	3	103	596
	4	97	562
	5	140	811
	6	174	1,008
3	1	219	1,271
	2	103	596
	4	144	834
	5	203	1,179
	6	270	1,564
4	1	154	893
	2	97	562
	3	144	834
	5	60	348
	6	153	887
5	1	150	872
	2	140	811
	3	203	1,179
	4	60	348
	6	113	655
6	1	95	549
	2	174	1,008
	3	270	1,564
	4	153	887
	5	113	655

Table 2. Lower Mantle Inputs to OEDIPUS.

Ra_{surf}	*avis*	ΔT (K)	η_0 (Pa·s)	H_s	Boundary
0.1008	20	500	10^{20}	10	Free Slip
40313	4	225	10^{21}	18	Free Slip
40313	4	225	10^{21}	0	Free Slip

Table 3. Plume Definition Test Case Inputs.

Run*	Ra_{surf}	ΔT (K)	η_0 (Pa·s)	H_s	Boundary
A†	0.055159	1140	10^{21}	5	No Slip
B	0.552	1140	10^{20}	5	Free Slip
C	0.552	1140	10^{20}	10	Free Slip
D‡	0.070919	1466	10^{21}	0	No Slip

*All runs are at *avis* = 20.
†Run A is not a low bottom viscosity case but has a large internal heating value and thus behaves similarly to Runs B and C.
‡Run D is a high bottom viscosity and low internal heating case for comparison.

Table 4. Plume Definition Results (organized in chronological order by definition).

Method*	P_f	Run A		Run B		Run C		Run D	
		Hot Plume #	*Cold Plume #*	*Hot Plume #*	*Cold Plume #*	*Hot Plume #*	*Cold Plume #*	*Hot Plume #*	*Cold Plume #*
1†	-	0	24	24.5	41	38	9.5	5	4
1, 20%	-	19.5	26.5	24	39	68.5	77.75	10	1
2†	-	-	-	23	30.5	41	72	-	-
3‡	5%	-	-	24	39	54	78	-	-
3	10%	-	-	22	39	37	78	-	-
4	5%	-	-	23	39	43.5	77	5	0
5	0.1%	-	-	13.25	18.25	0	7	-	-
6	5	-	-	22	38.5	7.5	56	-	-
6	10	-	-	18.25	33.5	3	28.5	-	-
6	15	0	9.5	15.75	25.5	0	8.5	5	0
6	20	-	-	13.5	14	0	2.5	-	-
7	-	0	10.5	1.5	4.25	0	0	4	1
8	5%	44	25.5	24	39	62.5	79	4	1
9	5	23.5	26.5	20.5	39	11.75	65	4	4
9	10	-	-	21.5	38	11	45	4	0
9	15	-	-	20.5	33.5	9	27.5	4	0
9	20	-	-	19	31	8	13	4	0

*Not every method was tried for every run.
†40% temperature or velocity difference.
‡Every method starting with this uses a 20% temperature difference except Method 4, which has a 20% velocity difference.

Acknowledgments

This research was carried out at the Jet Propulsion Laboratory, California Institute of Technology, and was sponsored by the USRP program and the National Aeronautics and Space Administration. I would like to thank Christophe Sotin and Sue Smrekar for mentoring me this summer, and my fellow intern Henry Tom for always being willing to count plumes.

References

[1]Smrekar, Suzanne E., et al. "Recent Hotspot Volcanism on Venus from VIRTIS Emissivity Data," *Science* **329** (2010): 605-608.

[2]Smrekar, Suzanne E. and E. Marc Parmentier. "The interaction of mantle plumes with surface thermal and chemical boundary layers: Applications to hotspots on Venus," *Journal of Geophysical Research* **101** (1996): 5397-5410.

[3]Kumagai, Ichiro, Anne Davaille and Kei Kurita. "On the fate of thermally buoyant mantle plumes at density interfaces," *Earth and Planetary Science Letters* **254** (2007) 180-193.

[4]Kumagai, Ichiro, et al. "Mantle Plumes: Thin, fat, successful, or failing? Constraints to explain hot spot volcanism through time and space," *Geophysical Research Letters* **35** (2008): 1-5.

[5]Choblet, Gaël. "Modelling thermal convection with large viscosity gradients in one block of the 'cubed sphere'," *Journal of Computational Physics* **205** (2005): 269-291.

[6]Parmentier, E.M. and C. Sotin. 'Three-dimensional numerical experiments on thermal convection in a very viscous fluid: Implications for the dynamics of a thermal boundary layer and high Rayleigh number," *Physics of Fluids* **12** (2000): 609-617.

[7]Sotin, C. and S. Labrosse. "Three-dimensional thermal convection in an iso-viscous, infinite Prandtl number fluid heated from within and from below: applications to the transfer of heat through planetary mantles," *Physics of the Earth and Planetary Interiors* **112** (1999): 171-190.

[8]Zhong, Shije. "Dynamics of thermal plumes in three-dimensional isoviscous thermal convection," *Geophys. J. Int.* **162** (2005): 289-300.